Journal of the Korean Nuclear Society
Volume 29, Number 4, pp. 280~290, August 1997

Robust Controller Design for the Nuclear Reactor Power Control System

Yoon-Joon Lee
Cheju National University
1 Ara-1dong, Cheju 690-756, Korea

Jung-In Choi
Kyungwon University
Bokjeong-dong, Seongnam City, Korea

(Received September 18, 1996)

Abstract

The robust controller for the nuclear reactor power control system is designed. The nuclear reactor is modeled by use of the point kinetics equations and the singly lumped energy balance equations. Since the model is not exact, the controller which can make the actual system robust is necessary. The perturbed plant is investigated by employing the uncertainties of the initial power level and the physical properties, and by introducing the delay into the modeled plant. The overall system is configured into the two port model and the H_∞ controller is designed. In designing the H_∞ controller, two factors of the loop shaping and the permissible magnitude of control input are taken into account. The designed controller provides the sufficient margins for the robustness, and the transients of the system output power and the control input satisfy their associated requirements.

1. Introduction

As a part of the overall improvements for the next generation nuclear plants, a great effort has been made to upgrade the control system by use of the digital technologies[1]. Particular emphases are laid on the more improved man-machine interface system for the operators such as control room design, signal processing, and plant communication systems. And in parallel with the use of digital hardwares, the softwares both for the process system and the protection system have drawn a great attention for the system reliability[2].

In the previous studies[3][4], the Wiener-Hopf-Kalman (WHK) techniques are applied to the design of the nuclear power control system. The results show that the WHK system has sufficient margins and a good tracking performance. But the WHK has the presumptions that the process plant be exactly described with no uncertainties and the stochastic properties of the noises be known. In the real world, this is impossible. During the modeling process, the assumptions for the simplifications and the linearization are almost inevitable, and the system is subject to change during the operation. The actual control system should endure all these uncertainties and variations, and it can be said that the purpose of the control system design is not the stability but the robustness [5].

The H_∞ optimal control technique provides an ef-

ficient tool which can deal with the modeling errors and external disturbances. In contrast with the WHK which stresses the performance only, the H_∞ control optimizes both the performance and the robustness, resulting in the meaningful optimizations. Since it is an optimization process in the frequency domain, the existing classical techniques can be used. In this paper, a robust controller is designed by use of the H_∞ theory for the nuclear reactor power control system. The reactor plant model is established by use of the one delayed neutron group point kinetics equations. The singly lumped thermal -hydraulic energy balance equations are incorporated to take account of the temperature feedback effects. Since this modeling assumes a linearization and the equations are simplified ones, the nominal model is different from the actual one. The perturbed model is set up by applying various kinds of uncertainties and its control characteristics are investigated. Then a two port model is established along with the system equations with which the H_∞ controller is designed. For the designed system, physical constraints are considered through the numerical simulations, and the controller is modified to meet these constraints.

2. Plant Modeling and Uncertainties

The reactor plant is modeled by use of the point kinetics equation and the singly lumped energy balance equations. The details, together with the nomenclatures, are fully described in Ref.[3], and only the briefs are presented in this paper. The one delayed neutron group point kinetics equations are applied to describe the reactor dynamics, and then linearized with the assumption of small perturbations to obtain the following equations.

$$\frac{d}{dt}\delta\overline{P} = \frac{\delta\rho-\beta}{\Lambda}\overline{P} + \frac{\beta}{\Lambda}\delta\overline{C} \tag{1}$$

$$\frac{d}{dt}\delta\overline{C} = \lambda\delta P - \lambda C(t) \tag{2}$$

where $\delta\overline{P}$ =normalized power variation $=\frac{\delta P}{P_0}$, $\delta\overline{C}$ =normalized precursor density variation $=\frac{\delta C}{C_0}$, ρ =reactivity, β =delayed neutron fraction, λ = precursor decay constant and Λ =neutron effective life time.

For the temperature feedback effects, the singly lumped parameter energy balance model is incorporated to the above equations. The reactivity acting on the plant is the sum of feedback reactivities and the external control effort.

$$\frac{d}{dt}\delta\rho = \frac{d}{dt}\delta\rho_x + \alpha_f\frac{d}{dt}\delta T_f + \alpha_c\frac{d}{dt}\delta T_c \tag{3}$$

where α_f =fuel temperature feedback coefficient,

α_c =coolant temperature feedback coefficient,

δT_f =fuel temperature variation,

δT_c =coolant temperature variation.

It is assumed that the reactivity worth of the control rod is constant through its length. Then the external control effort is

$$\frac{d}{dt}\delta\rho_x = V_r\frac{\rho_H}{H} \tag{4}$$

where V_r is the rod velocity (m/sec), ρ_H is the rod worth, and H is the rod length. All of these equations are put together to give the following state equation.

$$\dot{\mathbf{x}} = \mathbf{Ax} + \mathbf{Bu}$$

$$\mathbf{x} = (\delta\overline{P} \quad \delta\overline{C} \quad \delta T_f \quad \delta T_c \quad \delta\rho_x)^T \tag{5}$$

The system matrix **A** is of 5 by 5, and the input vector **u** has three elements of the coolant inlet temperature variation, coolant flow rate variation and the rod velocity. By assuming that the coolant inlet temperature and flow rate are constant, and the measured signal is the power only, the multivariable system of above equation is reduced to the SISO (single input single output) system. However, in the actual situation, there might be transients in coolant inlet temperature and reactor coolant flow rate. Also various signals are measured. Therefore, to reflect the more real situation, the system should be described in the MIMO (multi input multi output) system, and its corresponding controller design becomes

more difficult, whatever design technique might be used.

Since the system matrix **A** is the function of an initial power, the eigenvalues of the system vary with the initial steady power. Figure 1 shows the system eigenvalues of the plant for the various initial power levels, except that of an integrator. The physical values are quoted from the FSAR of Kori Unit 2[6]. As shown in the figure, the system is always stable. But with the decrease of the initial power, the most sensitive pole approaches to the original point and the plant becomes the system of a double integrator and a lead. The phase margin decreases from 105° for the full power to 87° for the zero initial power. This indicates that it is more difficult to control the plant when the initial power is low. Since the reactor plant of Eq.(5) is of minimum phase, it is possible to make the stable control system only with a unity feedback loop and a feedforward gain. However, because almost all of the root loci lie on the real axis of the complex plane, the damping coefficient is one. To improve the control characteristics of the system, it is desirable to locate the roots on the complex plane by controlling the feedforward gain. But at the lower initial power, the range of the feedforward gain which can make the system stable is very narrow, and there is a limitation if the control design is made by the feedforward gain with the unity feedback configuration.

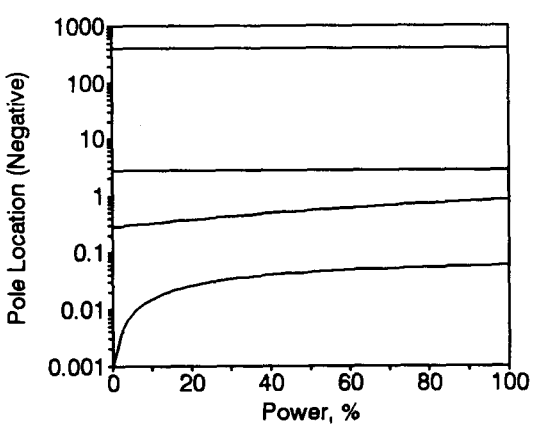

Fig. 1. Plant Eigenvalues by Initial Powers

The reactor model of Eq.(5) has an error. It arises from the equations employed in the modeling as well as from the assumptions used in Eq.(4). Although the nominal plant of Eq.(5) is always stable, the actual plant may not. However, it is difficult to estimate the difference quantitatively between the model of Eq.(5) and the more elaborate model which could be developed by the time dependent diffusion equations with the multi nodal thermal-hydraulic energy balance equations. Hence, the limitation included in Eq.(4) is used to estimate the uncertainties indirectly. In Eq.(4), it is assumed, for the purpose of linearization, that the differential rod worth is constant. But the differential rod worth is described more precisely by

$$\frac{d\rho}{dt} = \rho_H\left(1-\cos\frac{2\pi x}{H}\right)\frac{dx}{dt}/H \qquad (6)$$

The comparison between Eq.(4) and Eq.(6) shows that there is a delay of the control input in the modeling. Other sources of uncertainties are physical properties of the reactor. For example, the moderator temperature coefficient is subject to change with the boron concentration, and the fuel temperature coefficient is to change with the fuel temperature. The gap heat transfer coefficient has a value ranging from 2,000 w/m^2 ℃ to 11,000 w/m^2 ℃. All these uncertainties are assumed to be included in the perturbed plant. The physical data both for the nominal plant and the perturbed plant are shown in Table 1. These data are quoted from the FSAR of Kori Unit 2. For the perturbed plant, the data are determined in such a way to drive the system to the worst case in light of the system stability. Then the perturbed plant can be written as

$$\tilde{G} = G_p(s) \cdot D(s) \qquad (7)$$

where $G_p(s)$ is the plant with the worst physical data, and D(s) is the delay described in the second order equation by the Padè relation.

In general, the delay has a large effect on the system. All the systems have delays because of the initial torque load on the actuator, which may result in

Table 1. Physical properties of Nominal and Perturbed Plants

Property	Nominal Plant	Perturbed Plant
Mod. Temp. Coeff.	0 pcm/℃	+14.4 pcm/℃
Fuel Temp. Coeff	−3.7pcm/℃	−2.28pcm/℃
Gap Heat Tansfer Coeff	4,850 w/m²℃	2,000 w/m²℃
Control Input Delay	No	Yes

unstability. Figures 2 and 3 show the relations of gain margins and phase margins of the nominal reactor, respectively, with the control input delays for the system configured in the unity feedback. Since the plant varies with the initial power, various initial powers are considered. The figures show that the critical delay time for maintaining the stability becomes smaller as the initial power is lower. When the reactor is operated at the rated power, the critical delay time is 5.8 sec, but with the initial power of 10%, the critical delay time is about 2.5 sec.

To investigate the relations between the nominal and perturbed plants in more detail, the small gain theorem is applied. For the case of the initial power of 90%, the nominal plant is obtained from Eq.(5), with the physical properties of Table 1, as below.

$$G(s)=\frac{228.5s^3+710.4s^2+229.1s+13.74}{s^5+406.3s^4+1450s^3+941.7s^2+48.87s} \quad (8)$$

By assuming that the initial power of the perturbed plant is 10% less than that of the nominal plant, and by applying the worst physical data of Table 1, with the delay of 4 seconds, the perturbed plant is

$$\tilde{G}(s)=\frac{117.5s^5+174.7s^4-346.8s^3}{0.5121s^7+208.8s^6+995s^5+1483s^4} \quad (9)$$
$$\frac{+131.5s^2+60.55s+3.775}{+981.5s^3+249.3s^2+10.87s}$$

Then the additive uncertainty and the multiplicative uncertainty are found to be as below.

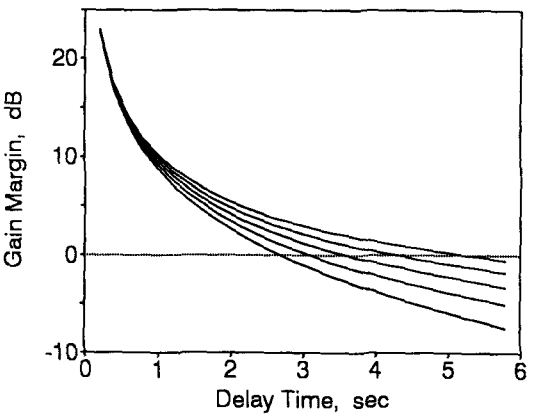

Fig. 2. Gain Margins by Delay Time (From top to bottom-100, 80, 60, 40 and 20%)

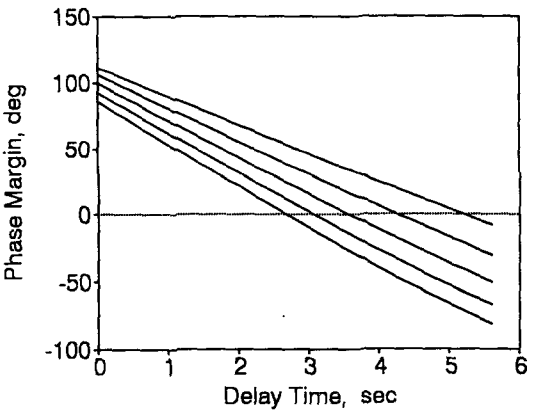

Fig. 3. Phase Margins by Delay Time

$$\Delta a=\tilde{G}(s)-G(s)$$
$$=\frac{0.029s^9+708.4s^8\ldots-1168s-68.6}{s^{11}+814.1s^{10}\ldots+1037s} \quad (10)$$

$$\Delta m(s)=\frac{\tilde{G}(s)-G(s)}{G(s)}$$
$$=\frac{0.0001269s^9+3.1s^8\ldots-5.114s-0.303}{s^9+407.8s^8\ldots+55.68s+1.577} \quad (11)$$

The small gain theorem says that the system is robust when the following conditions are satisfied.

$$|\Delta a|<\frac{1}{|K(s)(1+G(s)K(s))^{-1}|}=\frac{1}{|KS|} \quad (12)$$

$$|\Delta m| < \frac{1}{|G(s)K(s)(1+G(s)K(s))^{-1}|} = \frac{1}{|T|} \quad (13)$$

where S is the sensitivity and T is the complementary sensitivity.

Figure 4 shows the bode plots both of the nominal and perturbed plants. The magnitudes of the nominal and perturbed plants are almost the same each other, but the phase of the perturbed plant is less than that of the nominal plant. This indicates that the effect of the delay is the most significant among various sources of the uncertainty. The root locus diagrams, although not drawn here, show that the perturbed plant is of non-minimum phase because of the zeros located in RHP. Hence, there is a limitation on the upper boundary of the feedforward control gain (K=1.1096) for the perturbed plant, while there is no gain limitation for the nominal plant.

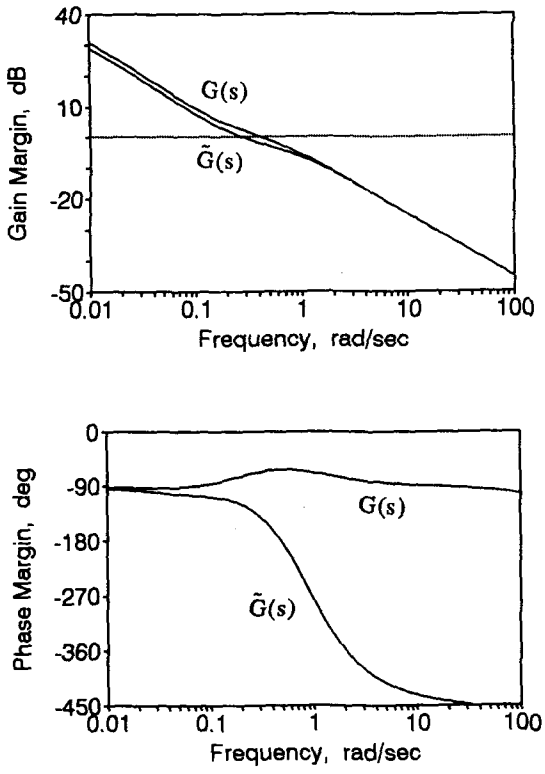

Fig. 4. Bode Diagrams of Nominal and Perturbed Plants

Figure 5 shows the singular values (SV) of the additive uncertainty and the return difference, and Fig. 6 of the multiplicative uncertainty and the inverse return difference, by letting K(s)=1. The robustness both for the additive and multiplicative uncertainties are verified from these figures. But there is neither the additive stability margin (ASM) nor the multiplicative stability margin (MSM), as can be known from the figures, and the time response of the system shows the marginal stability.

In addition to the output characteristics, the control input which acts on the plant should be considered for the control system design. If the designed control system is evaluated by the output responses

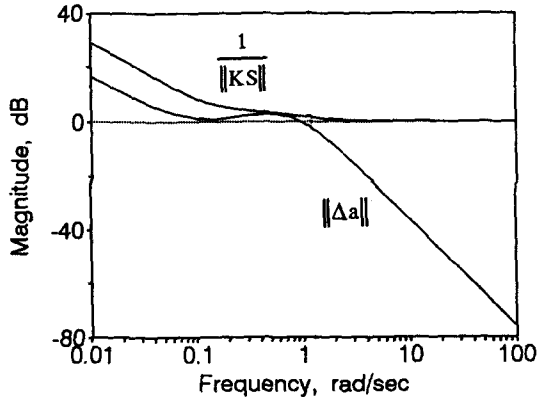

Fig. 5. Singular Value Plots of Additive Uncertainty and Return Difference

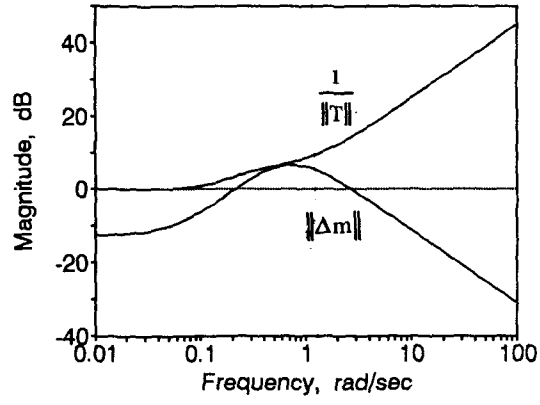

Fig. 6. Singular Value Plots of Multiplicative Uncertainty and Inverse Return Difference

only, the unity feedback system of the nominal plant, without any controller, can be a good system, and even the unity feedback system of the perturbed plant yields good characteristics if the delay is small. But the control input magnitude of the unity feedback system is very large both for the nominal and perturbed plants, which could not be permitted in the actual situation. Therefore, it is necessary to design a controller which satisfy the output tracking properties as well as the control input requirements.

3. H_∞ Controller Design

Figure 7 describes the reactor power control system. The controller K(s) which is to be designed is located on the feedforward loop. The disturbance, d, acts on the plant, and the measurement noise, n, on the feedback loop. The system of Fig. 7 is redrawn into the two port model of Fig. 8. The two port model consists of **P**(s) and K(s). **P**(s) has the multi inputs of exogenous vector **w**, say, the model uncertainty and measurement noise, and the control effort u. It has the multi outputs of plant output y_p and u. The reasons of including u in the outputs are to impose a limitation on the magnitude of the control input and to meet the rank condition for the existence of the H_∞ controller.

By defining the system input and output vector as **w** and **z**, respectively, the system described in Fig. 8 could be written in the following state equations.

$$\begin{aligned} \dot{\mathbf{x}} &= \mathbf{A}\mathbf{x} + \mathbf{B}_1\mathbf{w} + \mathbf{B}_2\mathbf{u} \\ \mathbf{z} &= \mathbf{C}_1\mathbf{x} + \mathbf{D}_{11}\mathbf{w} + \mathbf{D}_{12}\mathbf{u} \\ \mathbf{y} &= \mathbf{C}_2\mathbf{x} + \mathbf{D}_{21}\mathbf{w} + \mathbf{D}_{22}\mathbf{u} \end{aligned} \tag{14}$$

where $\mathbf{w} = (\mathrm{d}\ \mathrm{n})^T$, and $\mathbf{z} = (y_p\ \mathrm{u})^T$.

In the above equation, the system matrix **A** and the vector $\mathbf{B}_2$ are obtained from the plant, and other system matrices or vectors are as below.

$$\mathbf{B}_1 = \begin{pmatrix} 1 & 0 & 0 & 0 & 0 \\ 0 & 0 & 0 & 0 & 0 \end{pmatrix}^T, \quad \mathbf{C}_1 = \begin{pmatrix} 1 & 0 & 0 & 0 & 0 \\ 0 & 0 & 0 & 0 & 0 \end{pmatrix},$$
$$\mathbf{D}_{11} = \begin{pmatrix} 0 & 0 \\ 0 & 0 \end{pmatrix}, \quad \mathbf{D}_{12} = \begin{pmatrix} 0 \\ 1 \end{pmatrix}, \quad \mathbf{D}_{21} = (0 \quad -1),$$
$$\mathbf{D}_{22} = 0, \quad \mathbf{C}_2 = (-1\ 0\ 0\ 0\ 0) \tag{15}$$

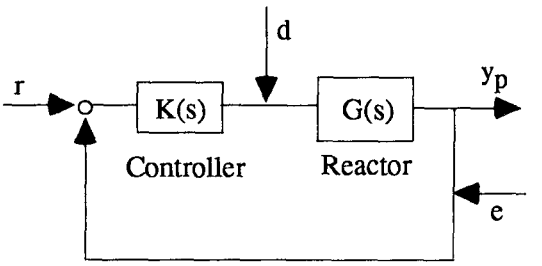

Fig. 7. Reactor Power Control System with Uncertainties

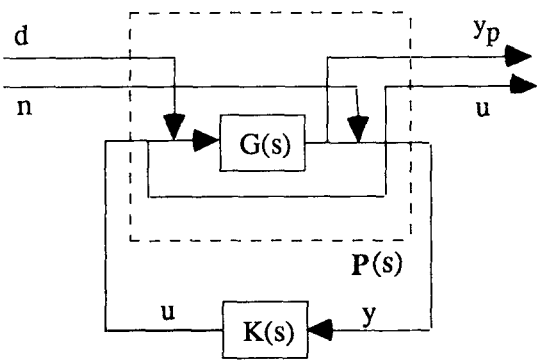

Fig. 8. Reactor Power Control System in Two Port Model

The H_∞ controller design is similar to the LQG design in that both are in the frame of Riccati equations. In the LQG, the controller is determined by separating the system into two subsystems of the optimal state feedback control law and the estimation problem. These two subsystems are described by the time dependent Riccati differential equations which are solved by forward or by backward progress. For the case of infinite horizon, the system equation is represented by the algebraic Riccati equations, whose solution can be easily obtained[8]. However, there is a fundamental difference between the H_∞ control and the LQG control. In the H_∞ control, the controller becomes different depending on how the exogenous signals act on the system. That is $\mathbf{B}_1$ of Eq. (14) has an effect on the controller for the H_∞ control, while it has an effect on the cost function only with-

out changing the controller for the LQG control. In addition, when a H_∞ filter is used to estimate the state variable, the estimated variable depends on the controller, which is not the case for the LQG Kalman filter. What makes the H_∞ controller more difficult is the conditions for the existence of the solutions. Contrary to the LQG problem, there is no guarantee that the Riccati equations of the H_∞ control always have the solutions.

The purpose of the H_∞ control is to design the admissible controller[9], that is well posed and has finite order, which makes the infinity norm of the overall closed loop system satisfy the following objective function.

$$\| R_{zw} \|_\infty < \gamma \tag{16}$$

The overall norm of the closed loop system $\|\mathbf{R}_{zw}\|_\infty$ can be expressed in terms of the linear fractional transformation which is defined as

$$\begin{aligned} \mathbf{R}_{zw} &= F_l(\mathbf{P}, \mathbf{K}) \\ &= \mathbf{P}_{11} + \mathbf{P}_{12}\mathbf{K}(\mathbf{I} - \mathbf{P}_{11}\mathbf{K})^{-1}\mathbf{P}_{21} \end{aligned} \tag{17}$$

where P_{ij} and $\mathbf{K}$ has the following relations.

$$\begin{pmatrix} z \\ y \end{pmatrix} = \begin{pmatrix} \mathbf{P}_{11} & \mathbf{P}_{12} \\ \mathbf{P}_{21} & \mathbf{P}_{22} \end{pmatrix} \begin{pmatrix} w \\ u \end{pmatrix}, \quad u = Ky \tag{18}$$

For the existence of the H_∞ controller, several conditions such as stabilizable and detectable, as well as the rank conditions for the system matrices regarding the order of input and output should be satisfied [10]. In addition, the existence of the $\mathbf{K}$ which satisfies Eq. (16) means that there is a solution of the following algebraic Riccati equation.

$$\begin{aligned} &X_\infty \tilde{A} + \tilde{A}^T X_\infty - X_\infty (B_2 B_2^T - \gamma^{-2} B_1 B_1^T) X_\infty \\ &+ \tilde{C}^T \tilde{C} = 0, \end{aligned} \tag{19}$$

$$\tilde{A} = A - B_2 D_{12}^T C_1, \quad \tilde{C}^T \tilde{C} = C_1^T (I - D_{12} D_{12}^T) C_1$$

For the reactor control system of Eq. (14), the H_∞ controller is determined by the above algorithms. As explained before, the H_∞ control has such a property that the controller becomes different depending on the way by which the exogenous signals act on the system. Hence, the H_∞ controller is designed by changing the state variable on which the disturbance acts from x_1 to x_1, that is, by changing the system matrix $\mathbf{B}_1$ as $\mathbf{B}_1 = \begin{pmatrix} 1 & 0 & 0 & 0 & 0 \\ 0 & 0 & 0 & 0 & 0 \end{pmatrix}^T$, $\mathbf{B}_1 = \begin{pmatrix} 0 & 1 & 0 & 0 & 0 \\ 0 & 0 & 0 & 0 & 0 \end{pmatrix}^T$, so on.

Table 2 summarizes the controller equation and the maximum value of the infinity norm of the overall system for each state variable which interacts with

Table 2. H_∞ Controller and Infinity Norm of the Overall System

Disturbance Injection State	Gain Margin dB	Phase Margin degree
x1	160	90
x2	–	–
x3	149	90
x4	181	90
x5	26	78

Table 3. Margins of the Unity Feedback System

Disturbed State	γ	H_∞ Controller
x1	80.19	$\frac{7.786\,10^{-4}s^3 + 3.04\,10^{-3}s^2 + 2.55\,10^{-3}s + 1.331\,10^{-4}}{s^5 + 398.6\,s^4 + 1569\,s^3 + 1412\,s^2 + 272.3\,s + 13.74}$
x2	No Solution	
x3	110.16	$\frac{1.12\,10^{-2}s^3 + 3.55\,10^{-3}s^2 + 1.331\,10^{-2}s + 2.\,10^{-4}}{s^5 + 406.5\,s^4 + 1536\,s^3 + 1258\,s^2 + 260.2\,s + 13.75}$
x4	88.57	$\frac{1.216\,10^{-4}s^3 + 4.21\,10^{-4}s^2 + 2.287\,10^{-4}s + 1.111\,10^{-5}}{s^5 + 406.7\,s^4 + 1593\,s^3 + 1418\,s^2 + 272.6\,s + 13.74}$
x5	0.0042	$\frac{9818\,s^4 + 3.989\,10^6 s^3 + 1.422\,10^7 s^2 + 9.255\,10^6 s + 4.82\,10^5}{s^5 + 564.2\,s^4 + 7.718\,10^4 s^3 + 2.351\,10^5 s^2 + 7.577\,10^4 s + 4544}$

the disturbance. And Table 3 shows the margins of the unity feedback system for each case.

When a disturbance acts on x_1, x_3, or x_4, the numerator of the H_∞ controller is very small. On the other hand, it is very large for x_5. The magnitude of the controller, or $\|\mathbf{K}\|_\infty$ more precisely, has direct effects on the system speed and other transient characteristics. The simulation for the two port system of Fig. 8 shows that the system is very slow for x_1, x_3 and x_4, and very rapid for x_5. This is also explained by the margins summarized in Table 3. When $\|\mathbf{K}\|_\infty$ is small, the gain and phase margins are excessively large. These excessive margins are beneficial to the system robustness, but they decrease the system performance. Figures 9 and 10 show the time responses of the output power and the control effort of the system for the unit step demand signal. The amplitudes of the figures indicate the relative magnitudes to the unit step input. The system is configured as a unity feedback system with the H_∞ controller located on the feedforward loop. From Fig. 9, for which the disturbance interacts with x_1, it can be known that the system speed is very low, and the control effort is very small. This indicates that the system has a poor performance with excessive robustness. Contrary to this, Fig. 10 (disturbance on x_5) shows the fast output response with a large control input.

These two extreme cases suggest that the performance and robustness can be traded off by controlling $\|\mathbf{K}\|_\infty$. There are two options in controlling $\|\mathbf{K}\|_\infty$. One is to increase $\|\mathbf{K}\|_\infty$ which is generated by acting the disturbance on x_1, the other is to decrease which is generated by acting the disturbance on x_5. To determine the proper one, the singular value (SV) plot of the overall closed loop system is considered. The singular value plot of each case is included in Figs. 9 and 10, respectively. The SV of the system with the disturbance on x_1 shows that the norm of the complementary sensitivity is small at low frequency. This indicates that the sensitivity of the system is large, which is vulnerable to the disturbance whose frequency is usually low. Further, the norm increases

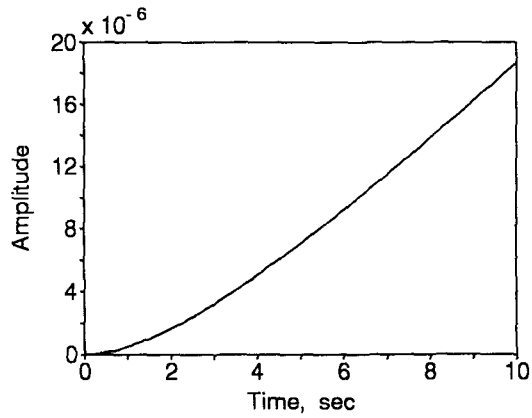

Fig. 9(a). Output Power of Closed Loop System

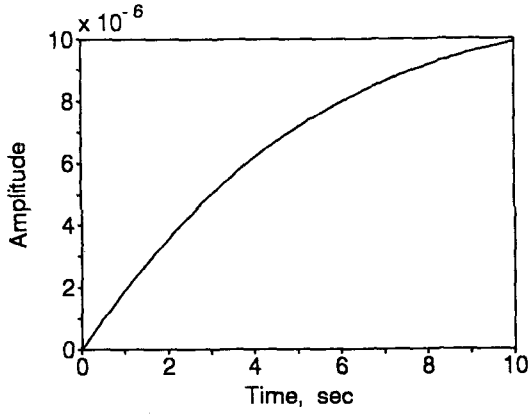

Fig. 9(b). Control Input of Closed Loop System

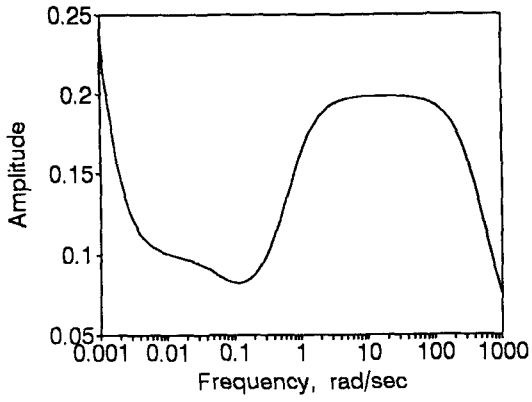

Fig. 9(c). Singular Value of the Closed Loop System

Fig. 9. Responses of Closed Loop System -Disturbance on x_1

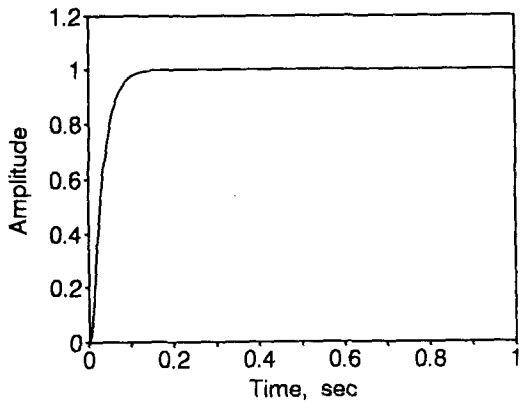

Fig. 10(a). Output Power of Closed Loop System

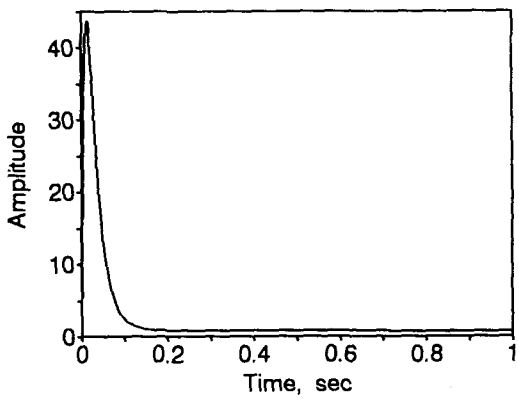

Fig. 10(b). Control Input of Closed Loop System

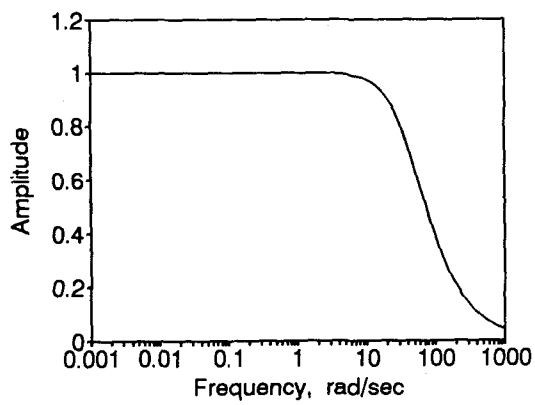

Fig. 10(c). Singular Value of the Closed Loop System

Fig. 10. Responses of Closed Loop System -Disturbance on xs

over the frequency range of about 10 to 10^3 rad/sec, which means the susceptivity to the noise. On the other hand, for the case of the system whose disturbance acts on x_5 (Fig. 10), the SV plot of the complementary sensitivity shows the conformity with the ordinary loop shaping, which provides the index of the design target. Therefore, the optimization is made by reducing $\|\mathbf{K}\|_\infty$ which is determined with the disturbance on x_5. And since the reducing of $\|\mathbf{K}\|_\infty$ results in the increase of margins, the system robustness can be improved furthermore.

The another factor to be considered is the magnitude of the control input, that is, the control rod speed. The maximum control speed is about 2cm/sec[6]. With this constraint on the control input, the controller is determined as below by the simulation using the utility program of MATLAB[11].

$$K(s) = \frac{22s^4 + 8939s^3 + 31856s^2}{s^5 + 564.2s^4 + 7.718\,10^4 s^3 + 2.351\,10^5 s^2} \frac{+20738s + 1080}{+7.577\,10^4 s + 4544} \quad (20)$$

With this controller, the gain margin increase from 26 dB to 78 dB, and the phase margin from 78° to 89° (see Table 3). The increase of the phase margin is particularly important in that it compensates the phase lag occurred by the delay.

Figure 11 shows the time responses of the output power and the control input as well, when the power is increased with step function from the initial level of 90% to 100%. As shown in the figure, the system output tracks the command signal within about 60 seconds, and the maximum control rod speed does not exceed 2 cm/sec which is set forth in the FSAR.

The FSAR also specifies that the overshooting should be less than 3% when the reactor is subject to a step increase from 90% to 100% power, and the system output satisfies this requirement. From the figure, the system speed seems to be somewhat slow. This is due to the limitation of the control input. If the permissible control rod speed is large, the system speed can be increased, of course.

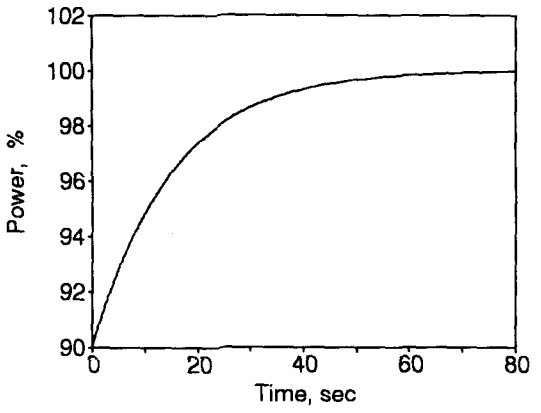

Fig. 11(a). Output Power Responses

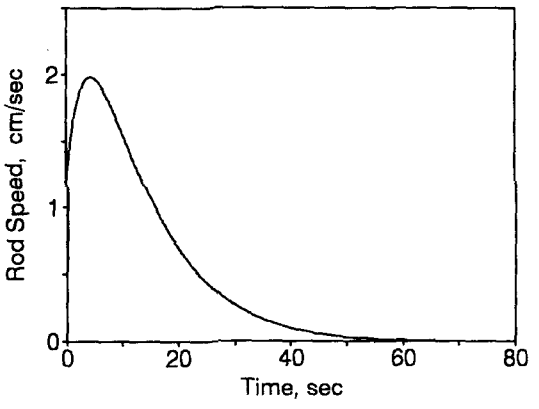

Fig. 11(b). Control Rod Speeds

Fig. 11. Output Power and Control Rod Speed of the Designed System

4. Conclusions

The plants to be controlled always have uncertainties which arise from the mathematical modeling description and the change of operating conditions, so on. Therefore, the actual control system should be robust with respect to these uncertainties. The H_∞ control technique provides the synthetical tool which considers both the robustness and the performance. To design the robust controller for the reactor power control system, the reactor is modeled by using the point kinetics equations and the singly lumped energy balance equations. Since the equations employed in modeling have limitations, the plant has uncertainties.

The feedback control system is configured into the two port model, and the robust controller is designed by use of H_∞ technique. The H_∞ controller depends on the way by which the exogenous signals act on the system. Hence, H_∞ controllers are designed by changing the state variable which interacts with the external disturbance. The control characteristics and the time responses for each controller are investigated. Then by modifying the infinity norm of the controller, with the constraint of the control rod speed, the H_∞ controller for the reactor control system is determined.

The system which consists of the plant and the designed H_∞ controller has sufficient gain and phase margins of 78 dB and 89°, respectively, for the robustness. In addition, the singular value plot of the system shows the desirable loop shape, which indicates the capabilities of the disturbance rejection at low frequency and noise rejection at high frequency. The magnitude of the control input is less than 2cm/sec which is the permissible maximum rod speed in the FSAR.

In reality, since the commercial reactor has a large negative temperature feedback effect and small neutron leakage, there is no problem in the power control. However, the result of this study might be useful when there is a large reactor property change due to the large power change or long term fuel burn up.

Acknowledgement

This paper was supported by the fund of Electrical Engineering & Science Research Institute.

References

1. *Integrated Instrumentation and Control Upgrade Plan*, Rev. 3, EPRI NP-7343 (1992)
2. *A Survey on the High Reliability Software Verification and Validation Technology for I&C in NPP*, KAERI/AR-411/94 (1994)
3. Y.J. Lee, "The Control Rod Speed Design for the Nuclear Reactor Power Control Using Optimal Control Theory," *J. of KNS*, **26**(4), 536-547 (1994)
4. Y.J. Lee, "A Conceptual Design of the Digital Nuclear Power Control System by the Order Increased LQR Method," *Proc. of NPIC & HMIT, ANS Int. Topical Meeting*, 827-834, Penn State Univ., Pennsylvania (1996)
5. P. Dorato (Ed.), *Robust Control*, IEEE Press (1987)
6. *Final Safety Analysis Report of Kori Unit 2*, 2nd ed., Korea Electric Power Corp (1989)
7. J.M. Maciejowski, *Multivariable Feedback Design*, Addison Wesley (1989)
8. F.L. Lewis, *Applied Optimal Control and Estimation*, Prentice Hall (1992)
9. M. Green, D.J.N. *Limebeer, Linear Robust Control*, Prentice Hall (1995)
10. T. Basar, P. Bernhard, H_∞ *Optimal Control and Related Minimax Design Problems*, Birkhauser (1991)
11. MATLAB, Ver. 4.0, Math Work Inc. (1992)